

Abstract

California Pellet Mill (CPM) manufactures steel ring dies for food pellet production and is considering induction hardening the interior of the passages. The feasibility of this method of surface hardening was evaluated by experiment and a simple model, which estimates transient temperatures in the die. Experimental results showed sufficient surface hardening, but the model suggested that the process is feasible only in dies in the larger end of sizes considered. The major constraint at smaller sizes is the cooling of the induction coil.

This work is sponsored by California Pellet Mill, Crawfordsville, IN.



Project Background

A proof of concept for a process improvement of steel ring dies from vacuum hardening to induction hardening was considered. The goal was to reduce cost by switching to 4140 steel, while maintaining a surface hardness of ~52 HRC for wear resistance and minimizing distortion.

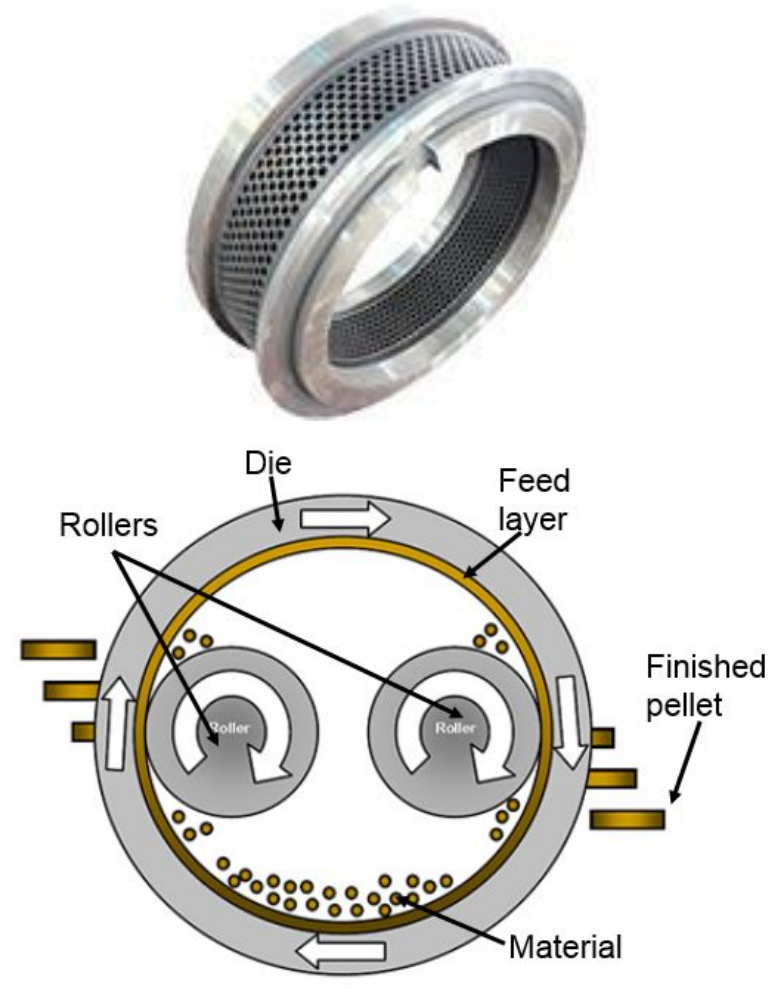


Figure 1. Steel ring die and a process schematic. "Ring Die." THE DESIGN OF PELLET MILL RING DIE, 4 Feb. 2017. www.biomass-energy.org/blog/pellet-mill-ring-die-design.html.

Induction hardening can harden a surface of a metal workpiece by inducing eddy currents and Joule heating in the metal through a time-varying magnetic field associated with the alternating current in a copper wire coil.

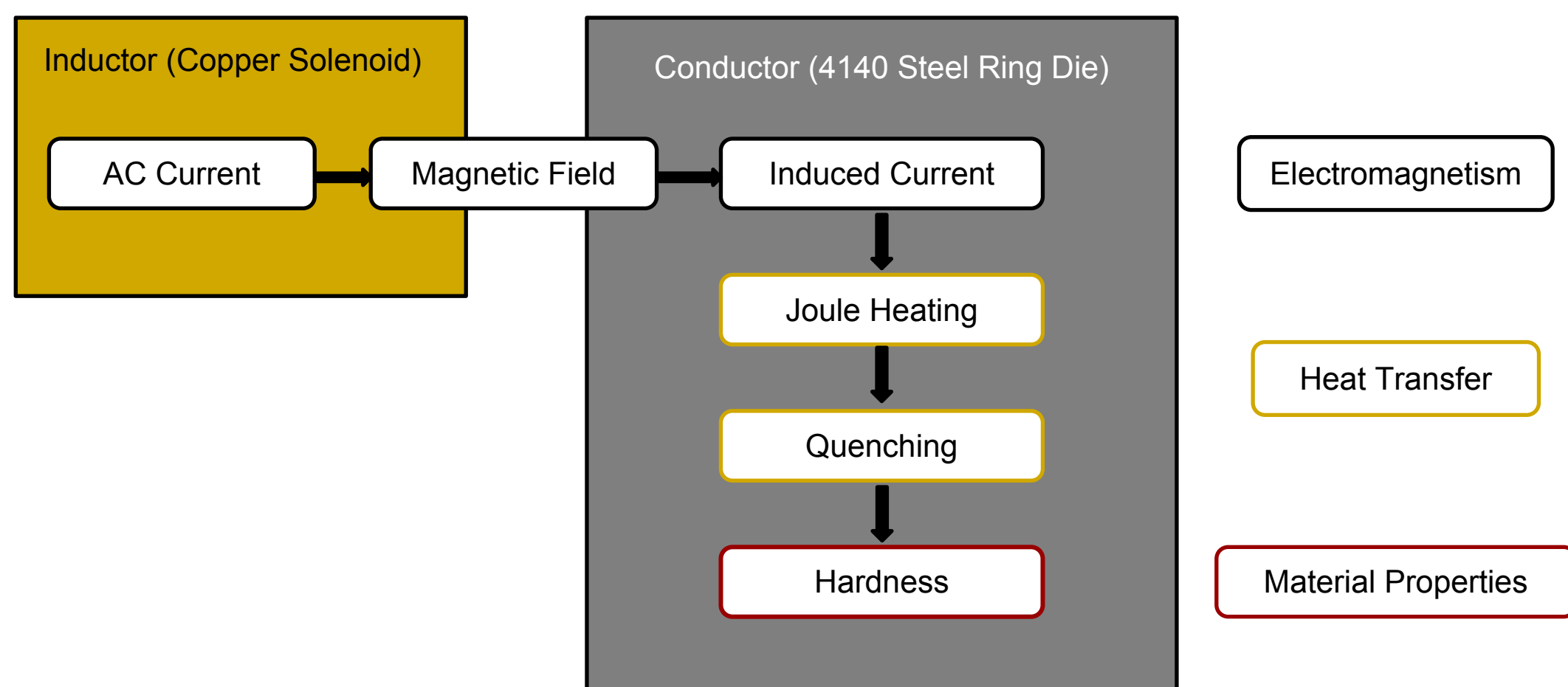


Figure 2. Schematic of induction hardening process.

Heat Transfer

The eddy current induced in the steel by the magnetic field generates heat, $q(r)$. The conduction in the steel was calculated by discretizing the conduction equation below using the finite volume method and solved with a 1D, transient tridiagonal matrix algorithm.

$$\rho c \frac{\partial T}{\partial t} = k \frac{1}{r} \frac{\partial}{\partial r} \left(r \frac{\partial T}{\partial r} \right) + \dot{q}$$

$$\dot{q} = C_o \frac{32 f^2 \mu_o^2 R_{HP}^4 P}{R_{es} \rho_{st} L^2 \pi} \left(\frac{2x}{r^2} + \frac{x^3}{4r^4} \right)^2 \left(\frac{2\pi^2 f + \sin(2\pi^2 f)}{8\pi f} \right) e^{-2\left(\frac{r-R}{R+\delta}\right)}$$

Results / Discussion

Sample Characterization

Optical microscopy confirmed that the required case depth was hardened to martensite, while verifying that quenching was needed to attain that martensitic transformation.

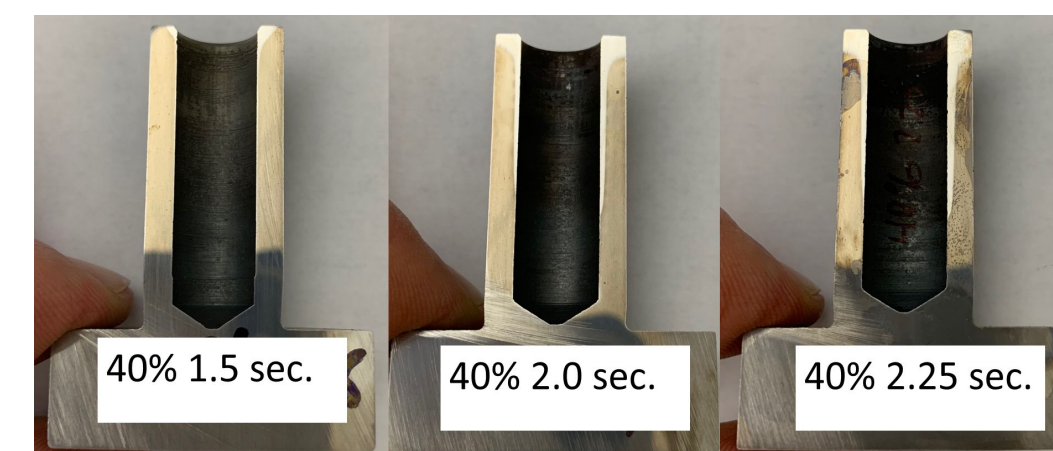


Figure 8. Pictures of Nital etched post-hardened samples A, B, and C with an inner radius of 0.009m and an outer radius of 0.015m.

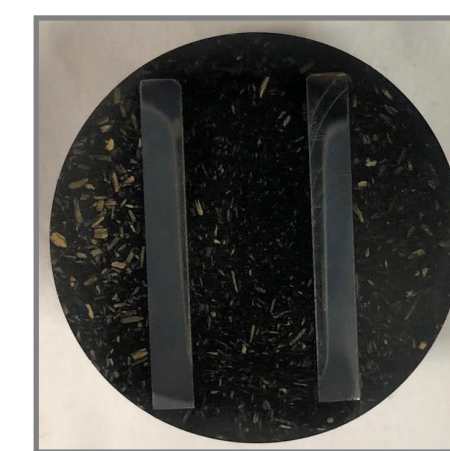


Figure 9. Mounted sample that shows the reflective hardened case depth.

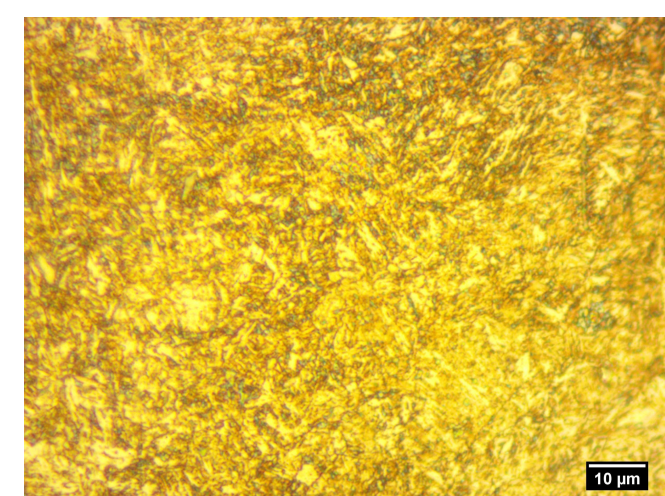


Figure 10. Representative micrograph of martensite after rapid cooling.

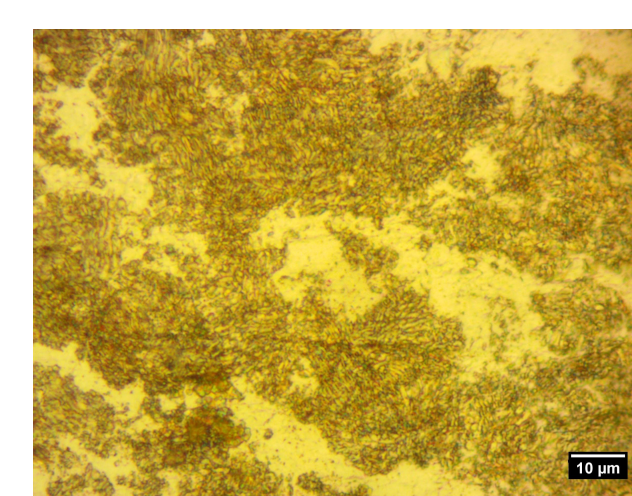


Figure 11. Representative micrograph of pearlite after slow cooling.

Table 1. Parameters set for samples A-F, each at 180 kHz frequency, along with case depths achieved.

Sample	Power (kW)	Time (s)	Case Depth (mm)
A	32	1.5	0.38
B	32	2.0	0.50
C	32	2.25	0.88
D	40	1.5	1.0
E	40	2.0	1.1
F	48	1.0	0.75

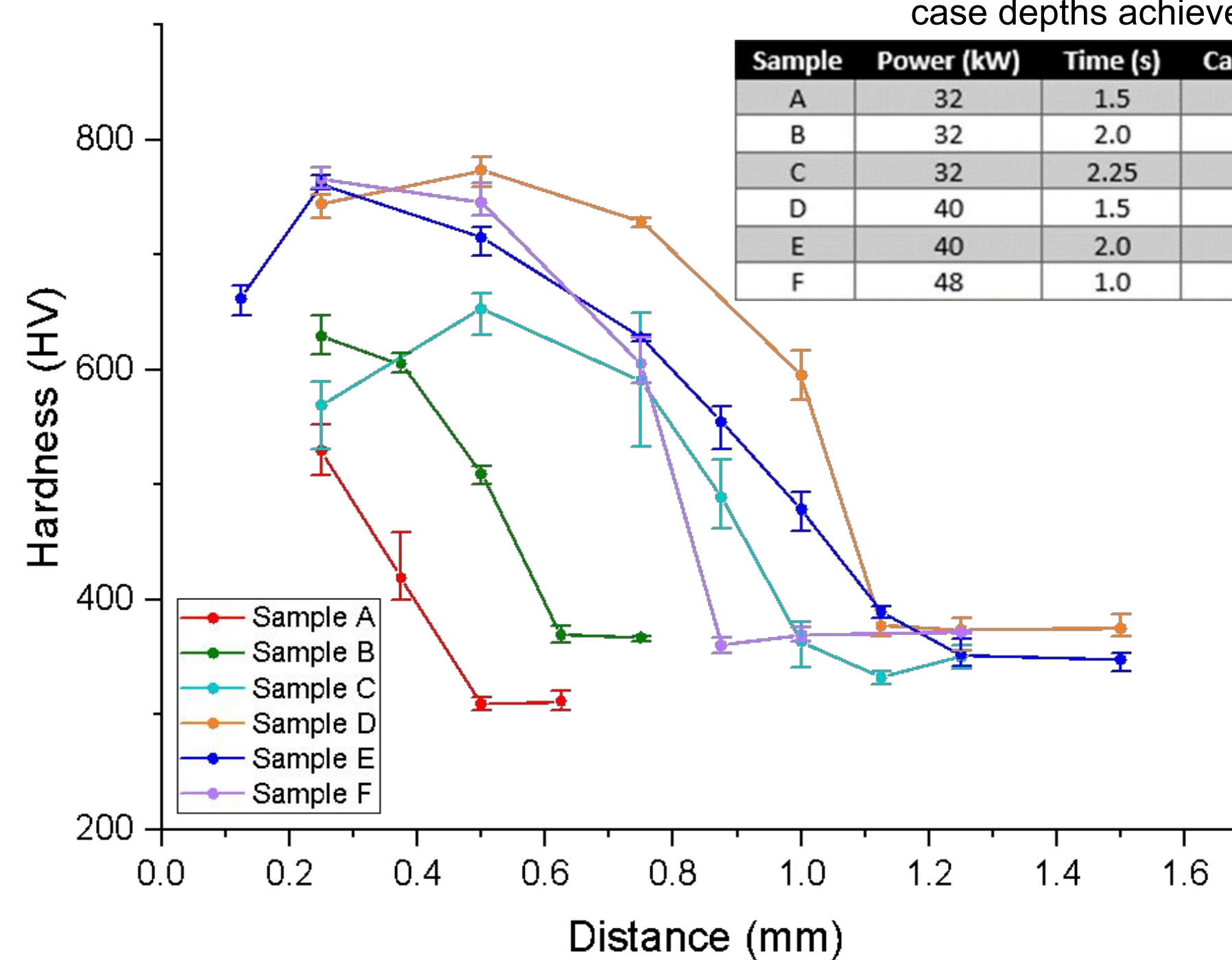


Figure 12. Hardness profiles from surface for samples A-F. Error bars represent the maximum and minimum measured values.

Quantifiable correlations between hardness, case depth, power, and time were found from experimental data:

- At 1.5 seconds, increasing power from 32kW to 40kW increases case depth by 163%.
- At 2.0 seconds, increasing power from 32kW to 40kW increases case depth by 125%.
- At 32kW, increasing time from 2.0 to 2.25 seconds, increases case depth by 75%.
- At 40kW, increasing time from 1.5 seconds to 2.0 seconds increases case depth by 12.5%.

Model

Radial temperature profiles around the die in the steel were found at different times. As time increases, the temperature increases until the power is shut off, then the temperature equilibrates in the sample before any quenching.

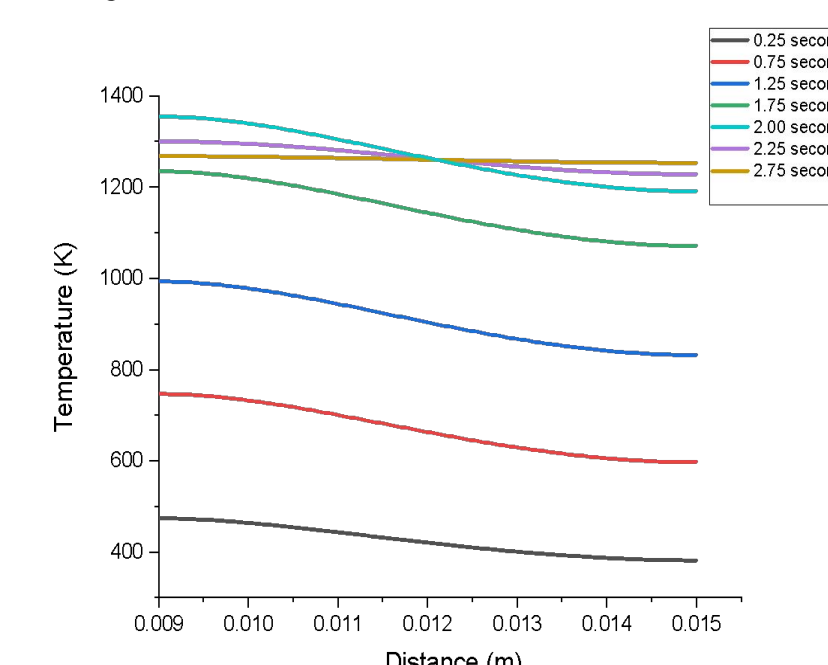


Figure 13. Temperature profiles at different times for sample B. The initial temperature is 300 K and the power is shut off at 2 s.

The trends depicted in the model for various powers and times are similar to those from the experimental data, but with different dependencies.

- As power and time increase, the surface temperature increases in the model, as seen in Figure 14.
- Generally, the higher the maximum surface temperature, the higher case depth, with the exception of samples B and D.
- As power increases with constant time, both the maximum surface temperature in the model and case depth in the experiment increase.
- As time increases with constant power, both the maximum surface temperature in the model and case depth in the experiment increase.

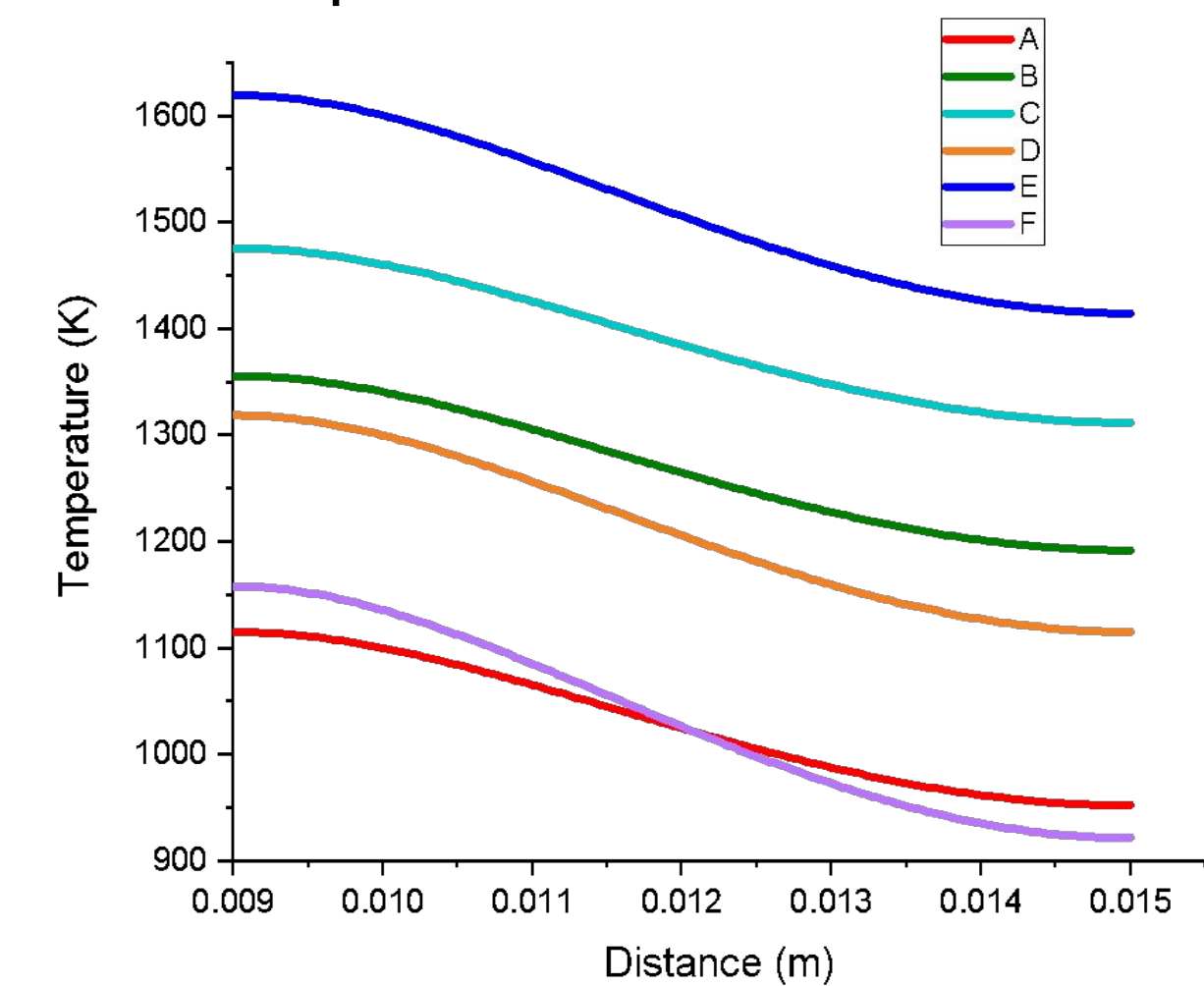


Figure 14. Temperature profiles as a function of distance from the surface (inner radius of 0.009m) at time of power shut-off.

Extrapolation of Results

The model of the hairpin coil was used to estimate system behavior with a 6mm diameter ring die hole. It predicted that:

- the necessary hairpin power to be 38W using C_o ,
- the surface temperature to be 6300 K and the exit coolant temperature to be 300°C, using a pump pressure of 1.2×10^6 Pa.

These conditions are obviously not practical, and so use of such a coil with a small diameter is most likely not possible.

Hairpin versus IRPC

- Compared IRPC calculated power (0.28W) to the hairpin coil power (38W)
- The IRPC requires 0.74% of the power in the hairpin

Experiments

The purpose of the experiments was to determine the viability of induction hardening a small hole with a hairpin coil. Pre-hardened 4140 steel samples were induction hardened with a 7.6 mm diameter hairpin coil, at different times and power levels at 180 kHz frequency.



Figure 3. Experimental hairpin coil.

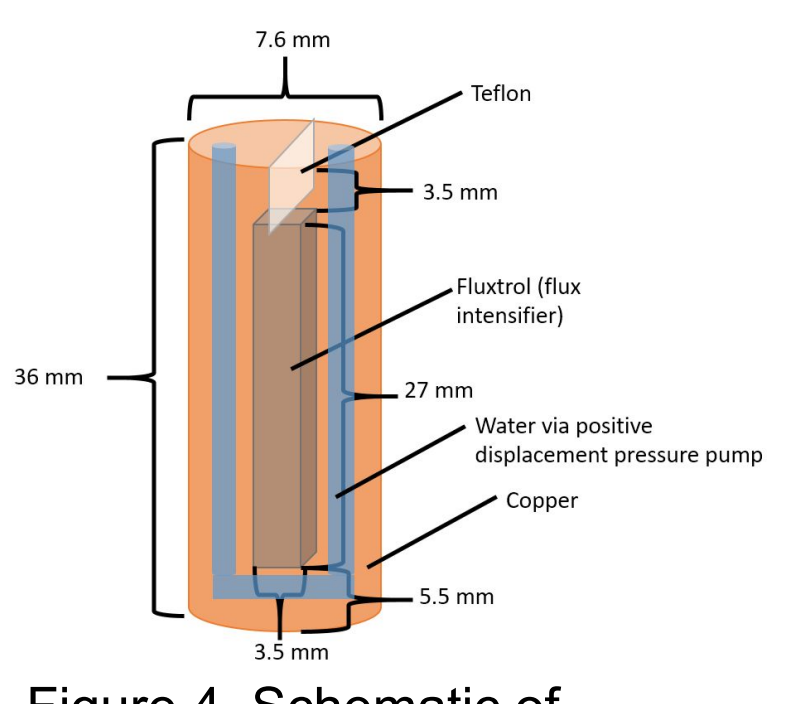


Figure 4. Schematic of hairpin coil.



Figure 5. Image of 180 kHz induction hardening machine at Contour Hardening.

Modeling

A model was developed to determine the feasibility of heating a ring die hole above austenization temperature and quenching to martensite for specified conditions. Two coil designs were considered: Figure 6a and 7a show a hairpin coil and Figure 6b and 7b an internal return pigtail coil (IRPC).

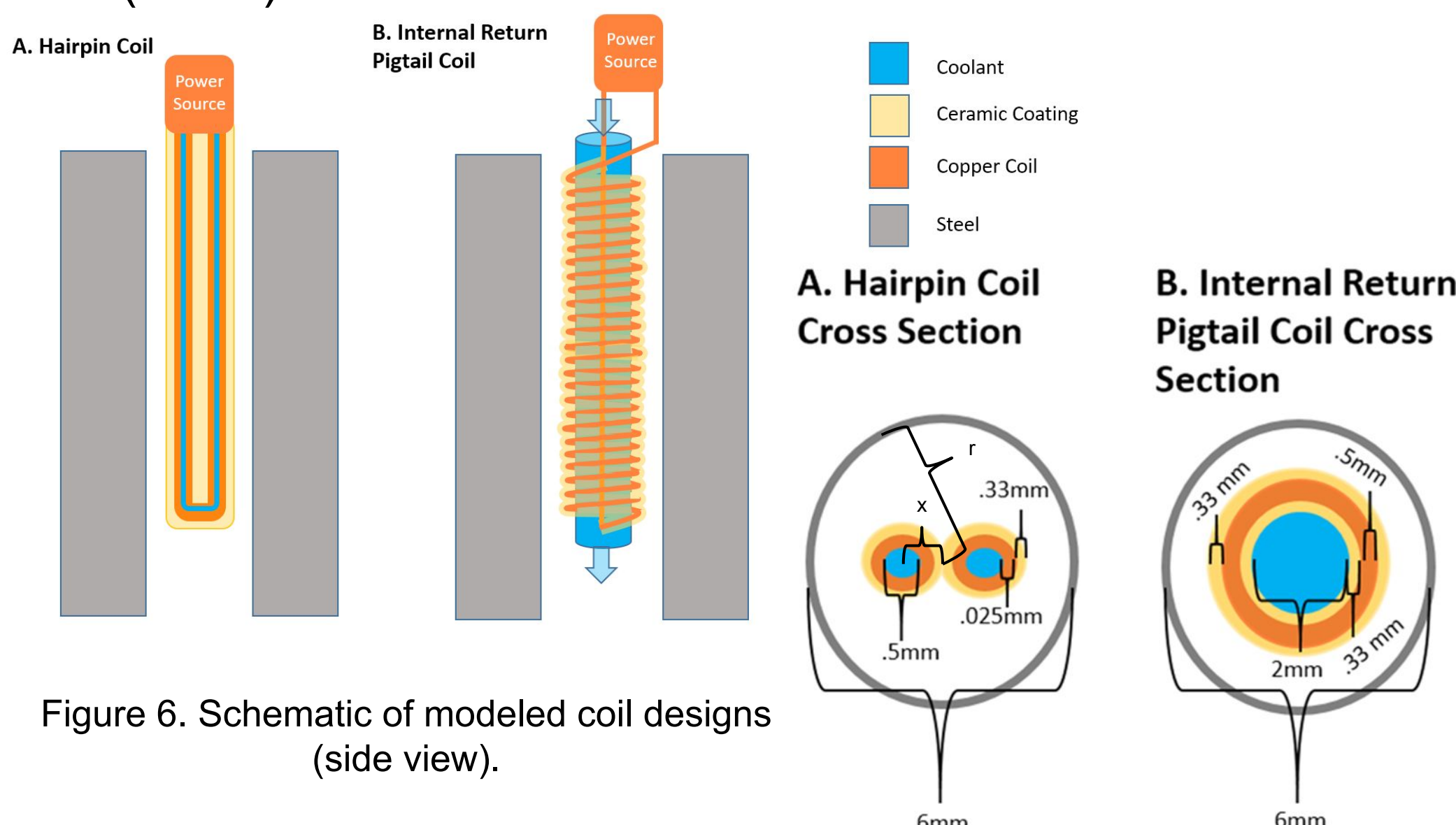


Figure 6. Schematic of modeled coil designs (side view).

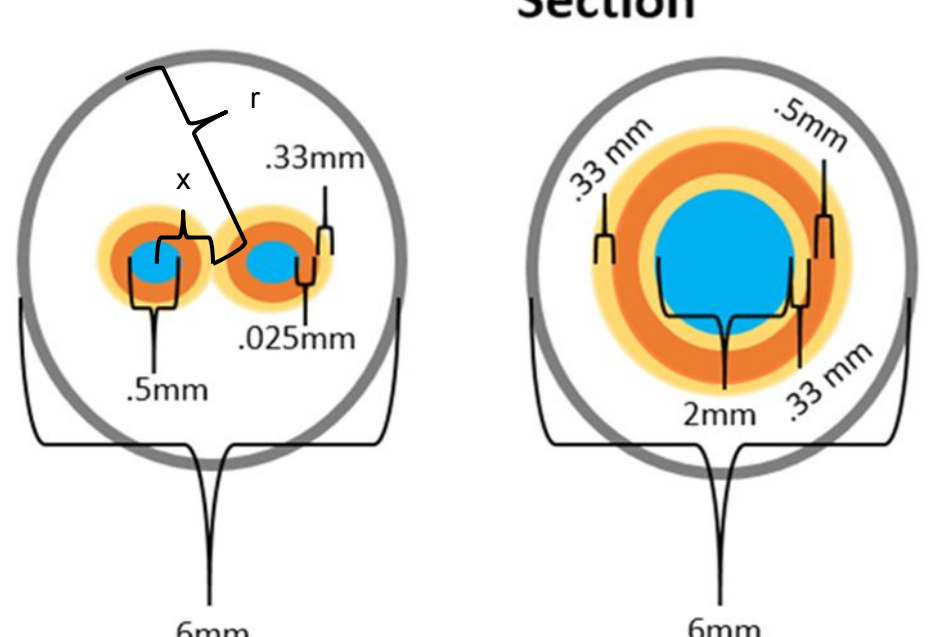


Figure 7. Schematic of modeled coil designs (top view).

Electromagnetism

An alternating current through a coil generates a time-varying magnetic field, which, in turn, causes a secondary current in the part. The magnetic field for a hairpin coil is:

$$B_{avg} = \frac{\mu_o I_{cu}}{\pi^2} \left(\frac{2x}{r^2} + \frac{x^3}{4r^4} \right)$$

Recommendations

It is recommended that CPM still continue to investigate induction heating with the IRPC design in figure 2b, as it would not require spinning and could produce more power. It is also recommended that flame hardening be considered, as it applies heat locally, but can be used in small passages without the constraint of coil cooling.

Future Work

- Tests should be run to validate the IRPC model
- Fabrication of coil design
- Flame hardening should be investigated as an alternative local hardening method
- Ability to spin the coil should be investigated
- Modeling in 2D to account for the flux intensifiers

Acknowledgements

We would like to thank Tom Kanaby from CPM, Kyle Hummel from Contour Hardening, Prof. Matthew Krane from Purdue University, and David Lynch from Induction Tooling.

References

- Incropera, F. P., & DeWitt, D. P. (2002). Fundamentals of Heat and Mass Transfer. New York: J. Wiley.
- Rudnev, Valery Totten, George E. (2014). ASM Handbook, Vol. 04. ASM International.